EXPERIMENTAL STUDY ON FLAME GEOMETRIC OF HORIZONTAL JET FIRE INPINGING A FACING WALL AND SIDE WALL

Youbo HUANG*, Bin WANG, Bingyan DONG, Ying TANG, Wenhe WANG

College of Safety Engineering,
Chongqing University of Science and Technology, Chongqing, China

* Corresponding author; E-mail: ybhuang@cqust.edu.cn

This work focuses on investigating the characteristics of restricted horizontal jet fire caused by fuel leakage as a pipeline or tank fracture. The study aims to quantify the effect of the exit velocity and nozzle-facing wall distance on the flame height and width, as well as developing a new non-dimensional heat release rate Q_n^* to better characterize the flame geometry. The study conducted three nozzle-facing wall distances (0.05, 0.10, and 0.15 m) with varying fuel ejection speeds from 1.04 to 6.25 m/s. Results show that the flame height and width increase with both the nozzle-facing wall distance and fuel ejection speed. The side wall constrains the air entering into the fire plume, which pushes the flame closer to the side wall. A new non-dimensional heat release rate Q_n^* was proposed on the basis of plate-nozzle distance, that the flame height and width fit well with the 1/4 and 2/5 power of Q_n^*, respectively. The global model was developed for flame size under multiple restrictions. The findings of this study are crucial in improving our understanding of the restricted horizontal jet fire accidents caused by fuel leakage and can aid in developing measures to minimize potential casualties and economic losses.

Key words: *jet fire, flame morphology, multiple wall, flame height, convective heat transfer*

1. Introduction

The demand for energy is increasing, and efforts are made to improve the efficiency of energy utilization while also exploring renewable energy sources to reduce the energy crisis and carbon emissions [1]. However, gaseous hydrocarbon fuel still plays an essential role in global energy usage [2]. Pipeline transportation and tank storage are key solutions for gaseous fuel utilization [3]. However, the broken pipeline or storage tank can cause fuel leakage, leading to jet fires, which are the most common accidents in the production, storage, and transportation of gaseous fuels in the chemical industry and urban residential areas [4]. In such incidents, the jet fire may be obstructed by obstacles such as surrounding tanks, pipelines, and buildings in industrial or dense urban areas (Fig. 1). This can result in a domino effect that can exacerbate the severity of the accident consequences. Historical surveys have shown that 50% of jet fires lead to a domino effect, which poses a significant challenge for energy utilization [5].

The geometry characteristics of impingement jet fire plays an important role for safety assessment and fire prevention [6], which has been extensively investigated. Most of the studies

focused on the vertical jet flame impinging on a ceiling [7,8] quantified the flame length of the vertical jet fire impinging on a horizontal ceiling, and proposed an empirical model on the basis of cylindrical or ellipse shape hypothesis. The inclination of ceiling is an important factor affecting the impingement jet fire characteristics [9] developed a global model for flame extension length along inclined ceiling, Wang *et al* [10] studied the flame extension length induced by a vertically impinging jet fire in confined compartment. As the complexity leakage condition, the jet fire is usually restricted by side wall or multiple obstacles. Hu *et al*. [11] proposed a non-dimensional model to predict the flame height of vertical jet fire constrained by two parallel side walls. Tao *et al*. [12] suggested that the air entrainment of jet fire are restrained by side wall, and proposed a correlation for total flame length of vertical jet fire bounded by a side wall and ceiling [13]. Considering the restriction of a side wall combined with ceiling, Zhang *et al*. revealed the flame extension length and developed an empirical model [14]. Up to now, the research on the flame length of vertical jet fire impinging on a ceiling is taken much attention, but there is not much research on horizontal jet fire impingement.

The initial momentum of vertical jet fire is in the same direction with the thermal buoyancy. The ceiling blocks the upward momentum of vertical jet fire and driven flame extended beneath the ceiling. However, for a horizontal jet fire, the direction of initial momentum is always perpendicular to the buoyancy force. The flame geometry under constrained boundary will significantly change as the interacting between horizontal momentum and thermal buoyancy [15]. Houf *et al* [16,17] and Schefer *et al*. [18,19] experimentally studied the hydrogen horizontal jet fire mitigated by different type of the barrier walls. Foroughi *et al*. [20] revealed the thermal effect of horizontal jet fire impinging on a parallel pipe. Wang *et al*. [10,21] conducted amounts of experiments for horizontal jet fire impinging on a facing plate to investigate the flame geometry and temperature profile. Huang *et al*.[22] developed an empirical model for flame extension height and temperature profile [23] based on the numerical results of horizontal jet fire impinging on a facing wall. Wang *et al*. [3] claimed that the flame extension length along vertical surface increased with the nozzle diameter and exit velocity, while a new correlation was developed for flame extension length. Tang *et al*. [24] used a curved surface imitating the tank to study the impinging behavior of horizontal jet fire on tank, and the flame height and width were correlated.

To summarize, previous research on jet fires has largely focused on the geometric characteristics of vertical jet fires and horizontal jet fires impinging only on facing wall. However, there is little investigation of horizontal jet fires that are constrained by multiple obstacles, such as a facing wall and a side wall, which is a common scenario in real-life accidents. In particular, there is a lack of quantitative data on the size of flames resulting from horizontally oriented jet fires impinging on multiple walls. The complexity of the impinging flow at corners, coupled effects of reduced air entrainment and buoyancy components along the sidewall, makes it difficult to quantify the flame length and width. Existing models are not suitable for predicting the flame size of a horizontal jet fires, which constrained by a front wall and a side wall. Given the diversity of real-life accident scenarios, there is a pressing need to develop simplified mathematical methods for predicting the behavior of horizontal jet fires restrained by multiple walls.

Therefore, this paper aims to better understand the flame geometry characteristics of horizontally oriented jet fires restrained by facing wall and a side wall. A series of experiments were carried out to quantify the flame length and width under different restricted conditions. The effect of nozzle-facing wall distance and fuel ejection velocity on flame size was analyzed. Based on theoretical

analysis and experimental results, a global model was established to predict not only the flame extension height but also the flame width under the constrained of facing wall and a side wall. This study provides significant reference to the disaster assessment and safety distance design for horizontal jet fires.

Figure 1. Schematic diagram of the horizontal jet fire, (a) freely horizontal jet flame, (b) impinging on facing wall and sidewall, (c) house building impinged by a jet flame

2. Experimental setup

In this work, the jet fire hits two obstacles both in the front direction and one side direction. Two square thermos-ability quartz glasses with dimension of 0.5 m were used to simulate the facing wall and side wall, as shown in Fig. 2. The conductivity of thermos-ability quartz is 1.4 W/(mK). The included angle between side wall and facing wall was 90°. The gaseous fuel is ejected horizontally and parallel to the side wall, and three different distances between the nozzle and the facing wall (0.05 m, 0.10 m, 0.15 m) are considered in present experiments. The distance between the nozzle and the side wall ($D_{n\text{-}s}$) is fixed as 0.05 m, and the nozzle is placed 0.14 m above the ground.

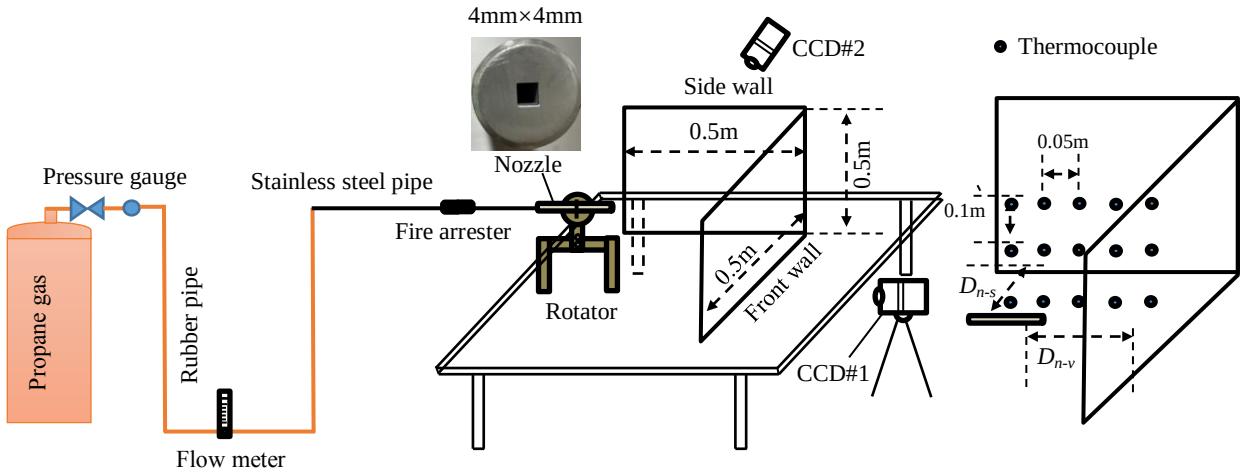

Figure 2. Schematics of experimental setup

The rectangular nozzle with dimension of 4 mm×4 mm was manufactured using stainless steel. The propane was used as the fuel. The combustion heat of propane is 46.4 MJ/kg [24]. The volumetric flow rate was controlled by the rotameter with the accuracy of ± 1.5%. Six flow rates from 1-6 L/min by an interval of 1 L/min were conducted. The corresponding fuel ejection velocity ranged with 1.04-6.25 m/s. The heat release rate of fire source varied in a range of 1.53-9.18 kW. The test conditions list in Tab. 1.

Two CCD cameras were installed to capture both frontal and side views of the flame shape. The resulting flame video footage was then processed using Matlab, with each frame being transformed into a pseudo-gray image. The probability of flame appearance was calculated by analyzing processed binary images at each pixel position. The flame occurrence probability of 50% was selected to determine the flame geometry [3]. The processing of flame image is shown in Fig. 3. Fifteen K-type thermocouples (diameter of 1mm, detected range of 100~1500 ℃, accuracy of 1 ℃) were evenly arranged to measure the flame temperature. Five thermocouple strings with three thermocouples in each string were installed along horizontal nozzle centerline. The horizontal distance between thermocouple is 0.05 m, and the vertical distance between each thermocouple is 0.1 m. The furthest thermocouple string was positioned along facing wall surface. The lowest thermocouple was placed at 0.08m above the nozzle.

Table. 1. Summary of test conditions

$D_{n\text{-}v}$ (m)	Volume flow (L/min)	Exit velocity (m/s)	$D_{n\text{-}s}$ (m)	Nozzle dimension
0.05, 0.10, 0.15	1, 2, 3, 4, 5, 6	1.04, 2.08, 3.13, 4.17, 5.21, 6.25	0.05m	4mm×4mm

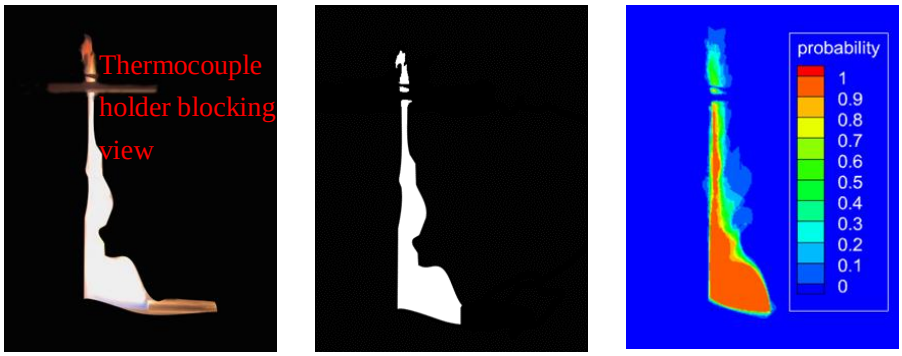

Figure 3. Schematic of the image processing

3. Results and discussion

3.1. Restrained flame geometry of horizontal jet fires

Figure 4 shows the typical side view of the jet flame with $D_{n\text{-}v}$ = 0.10 m. At relatively low initial velocities, the flame does not attach to obstacles because of insufficient initial momentum. The height of flame extension along the facing wall increases with larger fuel ejection velocities. At relatively high fuel jet velocity, more unburnt fuel impinges on the facing wall and being carried to higher elevations, resulting in a larger flame extension height. This qualitative change trend of the flame height is in consistent with previous horizontally impingement flame [21,24] .

At the horizontal region, the yellow and luminous flame gradually evolves to be blue and transparent, because of the mixing enhancement of unburnt fuel and air with larger velocity. This phenomenon is also identified with free jet fire conducted by Palacios *et al* [25]. The local Froude number Fr_{den} [26] in this study ranged of 8.9-53.8, and the Reynolds number *Re* [3] varied between 2810.8 and 16891.9. The jet flames in present experiments were mainly in buoyancy-dominated regime (Fr_{den} < 10) to momentum-dominated transition regime (10 < Fr_{den} <1000). With the increasing of fuel flow velocity, the jet flame transferred from up spread stage (no flame appearing below the

impingement stagnation point) to up-down spread stage (flame spreading downward the impingement stagnation point) with reference to impingement stagnation point. This is in consistent with previous study on the jet fire impinging a vertical plate [10]. Due to the extra restriction of side wall in this work, the critical jet velocity and nozzle-plate spacing for transition of horizontal flame morphologies is not applicable to the present bilateral restriction flame.

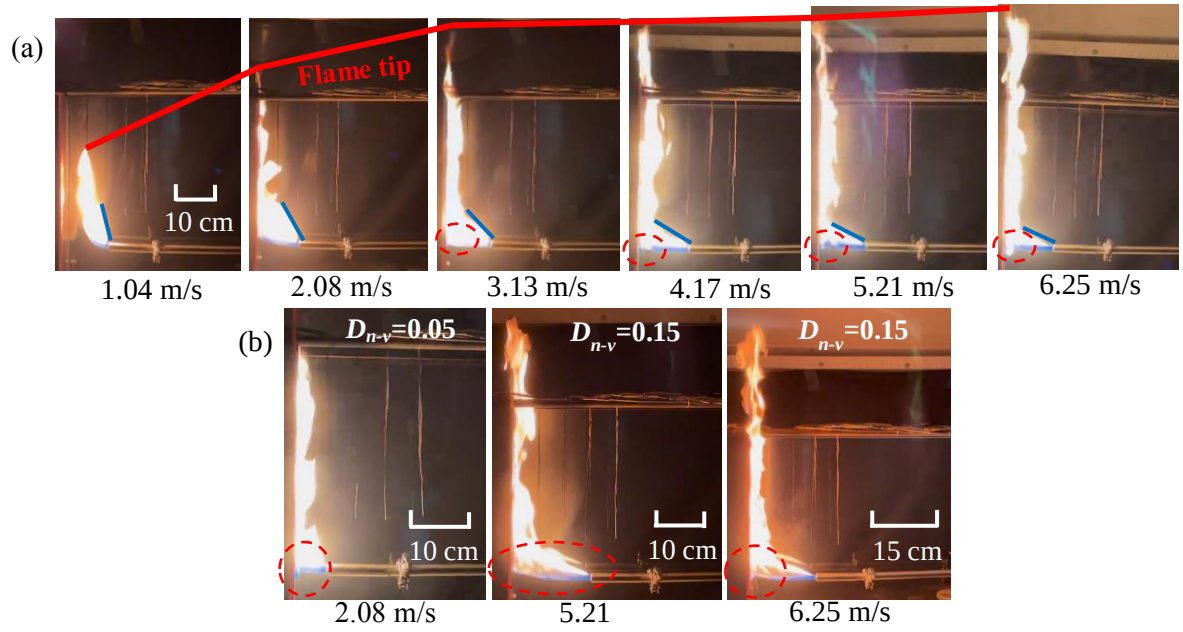

Figure 4. Typical flame morphology under different conditions, (a) Varied exit velocities with D_{n-v} = 0.10 m, (b) Nozzle-front plate distance 0.05 m and 0.15 m

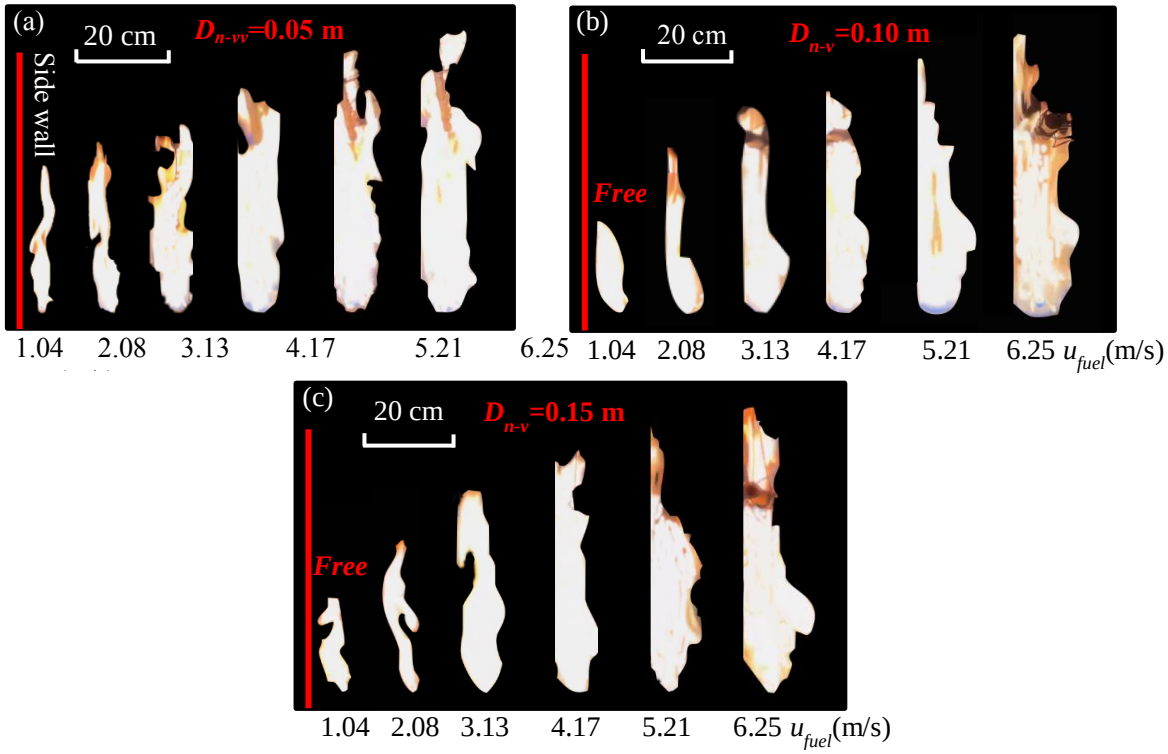

Figure 5. Front view of the typical flame, (a) D_{n-v}=0.05 m, (b) D_{n-v}=0.10 m, (c) D_{n-v}=0.15 m

Figure 5 shows the front view of the typical jet flame. As the fuel ejection velocity relatively large, the flame extends to the sidewall and below the impingement stagnation point. Under these

conditions, the relatively strong momentum flux causes the unburnt fuel to impinge on the vertical plate and extend transversely. The flame spans the finite distance between the nozzle and sidewall, and the trapping flame spreads over the sidewall surface. At relatively low fuel flow velocities, flame attaches to the sidewall only under small nozzle-facing wall distance. For a given test condition (D = 4 mm, $D_{n\text{-}v}$ =0.1 m, volume flow rate 4 L/min), the flame length in previous study on horizontal jet fire impinging on a curved surface was 0.329 m [24] less than present value of 0.506 m. When only one sidewall is present, blocking air entrainment in the transverse direction leads to an enlargement of the flame length along the vertical wall. When the fuel jet velocity was larger than a critical value (2.08 m/s), the flame reached the side wall, and the asymmetric flame morphology was emerged. A shorter nozzle-plate distance corresponded to a higher flame height.

3.2. Correlation for flame extension height and width

To facilitate the geometric description of the horizontal jet flame, the geometric size of jet flame defined as follows, (ⅰ) Flame extension height (h_v): the distance from the bottom edge of flame to the flame tip, (ⅱ) Flame width (h_w): an average of the width along the transversal direction [6]. Figure 6 shows the flame extension height under different conditions. The flame extension height increased as the initial fuel ejection velocity increased. However, the growth rate of the flame extension height was found to decrease when the fuel ejection velocity exceeded a critical value. This critical fuel ejection velocity for horizontal jet fire impinging on a curved surface and vertical plate were 6.25 m/s [24] and 10 m/s [21], respectively. In present study, the flame plume was not impinging on the barriers during jet velocity less than 3.13 m/s. Under this condition, the flame was not attached on the sidewall but bended to this side. Due to the presence of a sidewall, the entrainment and mixing of air with fuel are limited, causing unburnt fuel rising to higher elevations to mix with fresh air. Consequently, under relatively low fuel flow velocity, the flame height increases rapidly, but the growth rate slows down as momentum dominates and the flame thickness extends.

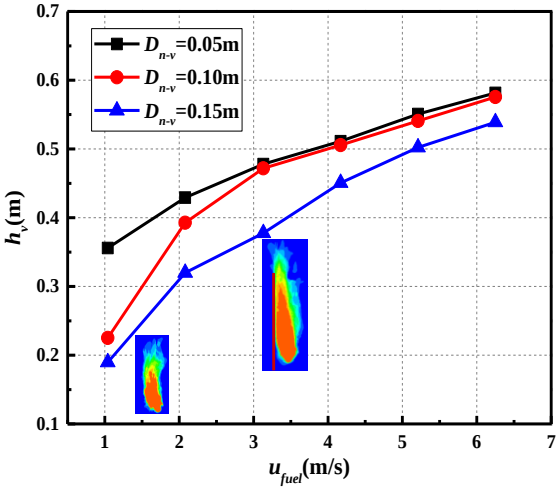

Figure 6. Variation of flame extension height under different conditions

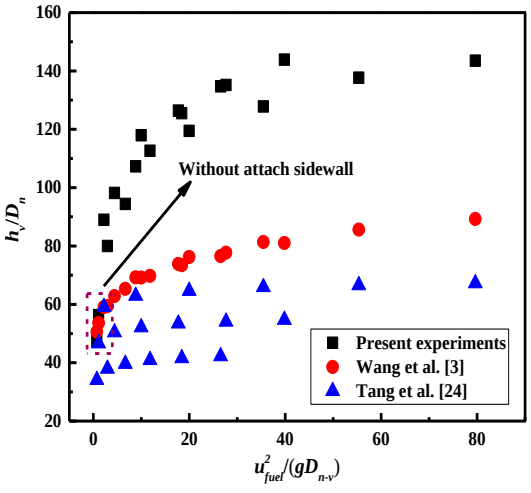

Figure 7. Non-dimensional flame height vs *Fr*

For a certain fuel ejection velocity, the flame extension height is reduced as larger nozzle-facing wall distance. Beyond a critical value of fuel ejection velocity (3.13 m/s), the flame extension height is largely independent of nozzle-facing wall distance. However, as the nozzle-facing wall distance increases to a considerable value, the flame extension height decreases significantly. The previous

study for horizontal jet fire impinging on a curved wall [24] and vertical plane [3] both found that the flame extension height persisted decline with nozzle-plate spacing. There are two reasons maybe useful for explaining this difference. First one is that the minimum spacing between nozzle and facing wall in previous study is less than this value in present work. Another one is that only one facing wall occurred in previous study but two obstacles in present work.

Figure 7 shows the relationship between the non-dimensional flame length h_v / D_n and Froude number $Fr = u_{fuel}^2$ / (g$D_{n\text{-}v}$), the predictions calculated by empirical model proposed by Wang *et al.* [3] and Tang *et al.* [24] are also plotted. The predictions are lower than the experimental results because of not considering the restriction of sidewall in previous model. Additionally, without attaching the sidewall, the predictions are closed to the experimental results. Thus, when the flame does not attach the side wall, the flame extension length along the facing wall can be predicted by using previous correction for impingement flame [3], expressed as Eq. (1):

$$\frac{H_{ef}}{D_{n-v}} = 455.82\left(\frac{D_{n-v}^3}{D_n^2 u_{fuel}^2}\right)^{-0.38}\left(\frac{Q}{\rho_\infty T_\infty c_p \sqrt{g} D_n^{5/2}}\right)^{-0.53} \quad (1)$$

where H_{ef} is the impinging flame height in m, $D_{n\text{-}v}$ is the separation distance between nozzle and vertical plate in m, D_n is the nozzle diameter in m, u_{fuel} is the fuel ejection velocity in m/s, Q is the heat release rate in kW, ρ_∞ is the ambient air density in kg/m^3, T_∞ is the ambient temperature in K, c_p is the specific heat in kJ/(kgK), g is the acceleration of gravity in m/s^2.

Currently, it is urgent to develop an advanced correlations capable of accurately predicting flame geometry for flame impinging on a facing and side wall. The horizontal flame has been cut in transversal direction during the nozzle-side wall distance less than half of the flame width (Fig. 8). Based on the continuity and axisymmetric distribution of the unburnt fuel after impingement, the mass equation can be expressed as $\dot{m}_u + \dot{m}_d = \dot{m} = 2\dot{m}_s$. Where $\dot{m}_u$ and $\dot{m}_d$ are the mass flow of the unburnt fuel in upward and downward, $\dot{m}_s$ is the mass flow of the unburnt fuel in transversal direction, $\dot{m}$ is the fuel mass just before impingement. At the impingement corner, the mass equation is given as $\dot{m}_v + \dot{m}_o = m_s'$. Where $\dot{m}_v$ and $\dot{m}_o$ are the mass flow of the unburnt fuel in vertical direction and opposite direction towards to the side wall, m_s' is the fuel mass in one side just before impinging on side wall, which relates to $\dot{m}_s$. The total mass flow includes ejected fuel and entrained air. The mass of the entrained air is given as $\dot{m}_e = 2\pi r u_e \rho d_D$, where $\dot{m}_e$ is mass flow of the entrained air, u_e is the entrainment velocity u_e=αu, α is the entrainment coefficient of 0.15, D is the horizontal distance away from nozzle.

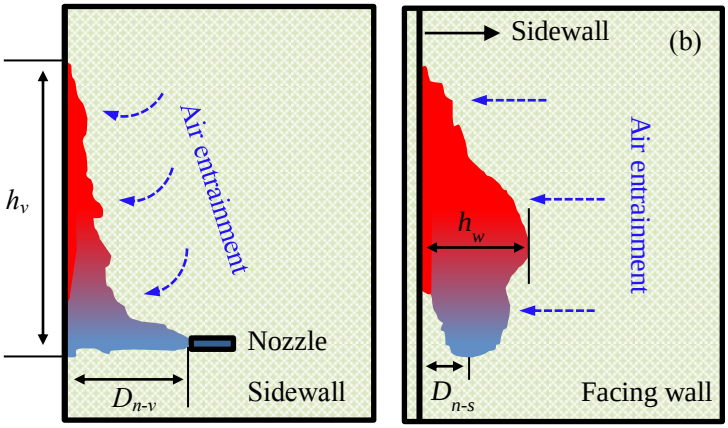

Figure 8. Schematic of horizontal jet flame impingement, (a) side view, (b) front view

Before impingement, the mass flow can be given as:

$$\dot{m} = \pi \rho_{fuel} D_n^2 u_{fuel} + \int_0^{D_{n\text{-}v}} 2\pi r \rho \alpha u dD \tag{2}$$

where ρ_{fuel} is the fuel density in kg/m^3, r is the radius in m.

The radius and flow velocity at interface between entrainment airflow and fuel jet can be predicted using follows equation [27]:

$$\frac{r}{D_n/2} = 3.4\left(\frac{0.1D}{D_n/2} + 0.294\right) \tag{3}$$

$$\frac{\partial}{\partial x_j}\left(\rho U_j k\right) - \frac{\partial}{\partial x_j}\left(\frac{\mu_{eff}}{\sigma_k}\frac{\partial U_i}{\partial x_j}\right) = G_{k_1} - \rho\varepsilon \tag{4}$$

where R is the radius of jet flame in m, y is the distance from y direction in m, u is the flow velocity in m/s, u_{max} is the maximum velocity in m/s.

Simplifying Eq. (4), the mass flow relates to one power of D_n and $D_{n\text{-}v}$. Physically, the unburnt fuel spreads upward as the buoyance component. The rate of momentum change must equal the buoyancy force per unit height over the height element $d(\dot{m}u)/dz = g \triangle \rho A$, where A is the area of mass flow, the density difference $\triangle\rho$ relates to the heat release rate $\triangle\rho = Q/(uAc_pT_\infty)$. Based on the energy change rate and buoyancy component, the mass flow of the unburnt fuel in upward is given as:

$$\dot{m}_u \sim f\left(\frac{V_{fu}}{V_f}Q\right) \tag{5}$$

The cut-off flame volume after impingement can be calculated using empirical model based on the assumption of elliptical cross-sectional [22]:

$$\frac{V_{fu}}{V_f} = \frac{V_f - C_1^2\frac{\pi}{3}D_{n-v}^3 - C_1(L+W)\frac{\pi}{4}D_{n-v}^2 - LW\frac{\pi}{4}D_{n-v}}{C_1^2\frac{\pi}{12}l_f^3 + C_1(L+W)\frac{\pi}{8}l_f^2 + LW\frac{\pi}{3}l_f} \tag{6}$$

where V_f is the volume of free flame in m^3, V_{fu} is the cut-off flame volume in m^3, L and W are the length and width of rectangular nozzle in m, C_1 is constant 0.325, l_f is the free flame length in m ($l_f/D_n = 22\mathrm{Fr}^{0.2}$).

The unburnt mass flow in transversal direction is given as:

$$\dot{m}_s \sim f\left(\frac{V_{fu}}{2V_f}Q\right) \tag{7}$$

The flame size is a function of unburnt fuel and air entrainment to consume this fuel after impinging on the vertical wall. The flame extends in a manner similar to a round disk from the impinging point under each direction [8]. The cross-section of the flame is assumed as ellipse shape due to the buoyance force, it gives:

$$\frac{V_{fu}}{V_f}u_{fuel}A_n\rho_{fuel}\Delta H_{c,fuel} \sim \pi h_v^2 u_e \rho_\infty \Delta H_c^{'} \tag{8}$$

$$\frac{V_{fu}}{2V_f}u_{fuel}A_n\rho_{fuel}\Delta H_{c,fuel} \sim \pi h_w^2 u_e \rho_\infty \Delta H_c^{'} \tag{9}$$

where A_n is the orifice area in m^2, $\Delta H_{c,fuel}$ is the heat of combustion per unit fuel mass in kJ/kg, $\triangle H_c'$ is the heat release per mass consumed air (2.91×10^3 kJ/kg), h_v and h_w are the flame extension height

and width in m. The air entrainment velocity relates to the buoyancy due to the gravitational acceleration and vertical distance $u_a \sim (gH)^{1/2}$. The Eq. (8) can be transferred as:

$$h_v \sim \sqrt{\frac{V_{fu}/V_f\, Q}{\pi\sqrt{gH}\,\rho_\infty \Delta H_c^{'}}} \tag{10}$$

The Eq. (9) is transferred as:

$$h_w \sim \sqrt{\frac{V_{fu}/V_f\, Q}{2\pi\sqrt{gH}\,\rho_\infty \Delta H_c^{'}}} \tag{11}$$

The nozzle-facing wall distance $D_{n\text{-}v}$ and nozzle-side wall distance $D_{n\text{-}s}$ influence the flame extension and air entrainment, which use to replace the dimension of H. Two sides of Eqs. (10) and (11) divided by hydraulic diameter of nozzle. The $\Delta H_c'$ relates to specific heat and temperature, it arrives:

$$\frac{h_v}{\left((D_{n\text{-}v}D_{n\text{-}s})^{1/2}D_n^4\right)^{1/5}} \sim \sqrt{\frac{V_{fu}/V_f}{\pi}Q_n^*} \tag{12}$$

$$\frac{h_w}{\left((D_{n\text{-}v}D_{n\text{-}s})^{1/2}D_n^4\right)^{1/5}} \sim \sqrt{\frac{V_{fu}/V_f}{2\pi}Q_n^*} \tag{13}$$

$$Q_n^* = \frac{Q}{\rho_\infty c_p T_\infty \sqrt{g(D_{n\text{-}v}D_{n\text{-}s})^{1/2}D_n^4}} \tag{14}$$

where Q_n^* is the dimensionless heat release rate.

Figure 9 shows the relation of normalized flame extension height and dimensionless parameter. The flame extension height can be well correlated, which gives:

$$\frac{h_v}{\left((D_{n\text{-}v}D_{n\text{-}s})^{1/2}D_n^4\right)^{1/5}} = 16.66\left(\frac{V_{fu}/V_f}{\pi}Q_n^*\right)^{1/4} \tag{15}$$

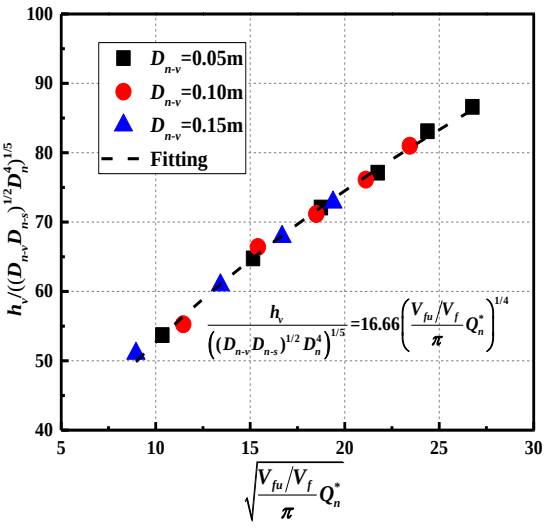

Figure 9. Dimensionless flame height vs dimensionless heat release rate

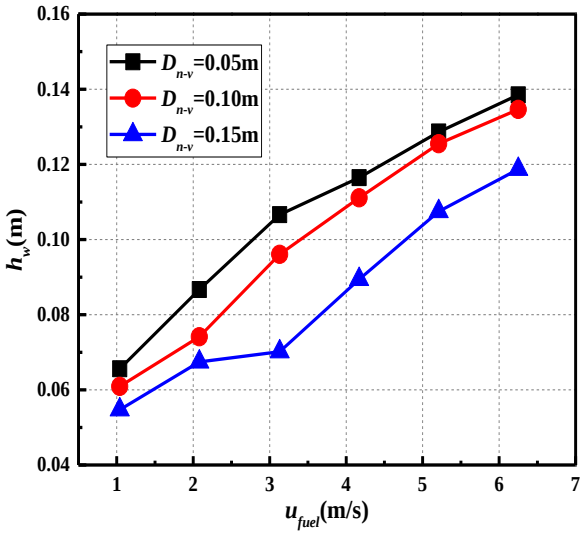

Figure 10. Flame width under different conditions

The flame width affects the heat radiation of jet fire to the surrounding facilities. Therefore, the flame width is evaluated as shown in Fig. 10. For a given nozzle-facing wall spacing, the larger fuel ejection velocity resulted in the wider flame. The lateral diffusion effect and air entrainment is

intensive under impinging condition. Thus, the width of impinging flame gradually increased. This is consistent with previous study of impingement jet flame [24]. But the flame width in present work is lower because of the constrained by a sidewall. Under a certain fuel ejection velocity, the flame width increased with the shorter $D_{n\text{-}v}$ as smaller cut-off flame volume.

Based on Eq. (13), the correlation between the dimensionless flame width and dimensionless heat release rate is shown in Fig. 11. The experimental data converges well to the fitting line. The predicted model for the flame width is given as:

$$\frac{h_w}{\left((D_{n\text{-}v}D_{n\text{-}s})^{1/2}D_n^4\right)^{1/5}}=2\left(\frac{V_{fu}/V_f}{2\pi}Q_n^*\right)^{2/5} \tag{16}$$

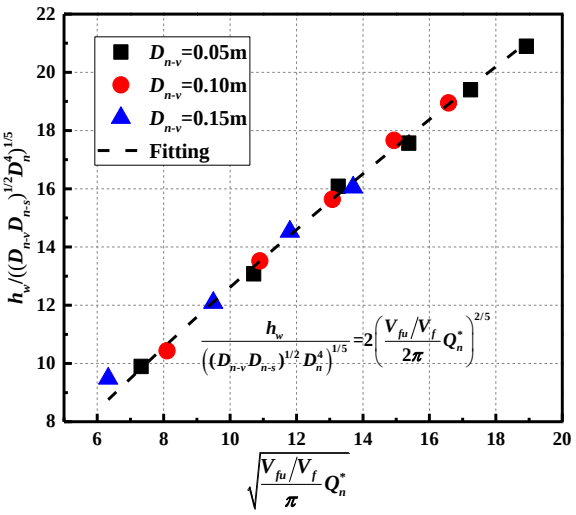

Figure 11. Dimensionless flame width vs dimensionless heat release rate

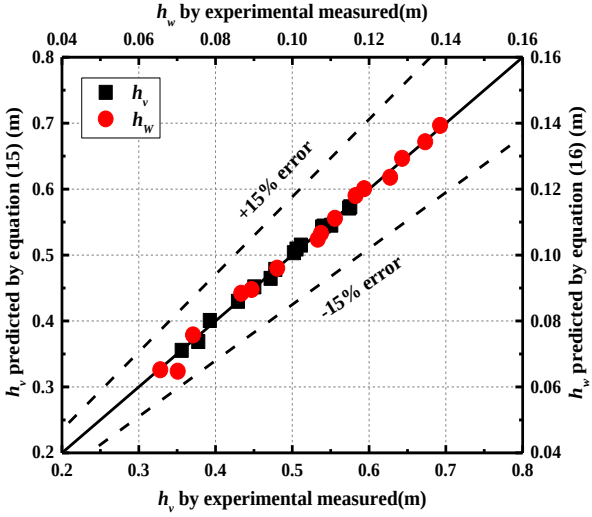

Figure 12. Comparison of predicted flame size and experimental data

Figure 12 shows the comparison of flame size predicted by proposed model with experimental results. The related errors of predicted flame extension length and width are lower than $\pm$15%. Totally, the predictions of flame extension length and flame width agrees well with the experimental results. Therefore, the developed model Eqs. (15) and (16) is reliable to predict the flame size of horizontal jet fire constrained by two obstacles.

4. Conclusions

This paper presents an experimental study on the flame extension height and width of horizontally oriented jet fires that hit both a facing wall and a side wall. The study includes a quantitative analysis to establish correlations between flame size and the characteristics of the horizontally restrained jet flame. The major conclusions are as follows:

The flame is sheared by a sidewall, while the flame is enlarged as the sidewall restricting the transversal extension. The vortex of flame appears below the impingement stagnation point that results in the blue flame at the lower edge.

The size of the flame is coupled to the initial velocity of the fuel and the nozzle-facing wall distances. Smaller nozzle-facing wall distances and larger initial fuel velocities can promote larger flame extension height and width. The flame dimension becomes more elongated under smaller nozzle-facing wall distances, but this trend decreases under small enough nozzle-facing wall distances.

A new dimensionless heat release rate (Q_n^*) was derived to correlate the flame size. This parameter considers the coupling effect of initial velocity, nozzle-plate distance both in the horizontal direction and transversal direction. New correlations show that the flame extension height increases linearly with $Q_n^{1/4}$, while flame width increases with $Q_n^{2/5}$. The proposed non-dimensional formula agrees well with experimental results of flame extension height and width.

Acknowledgment

This study was founded by the Natural Science Foundation of Chongqing, China [Grant No. cstc2021jcyj-msxmX0919], the Science and Technology Research Program of Chongqing Municipal Education Commission [Grant No. KJQN202101527], the National Natural Science Foundation of China (NSFC) [Grant No. 52104185], the Research Foundation of Chongqing for graduated doctor, [Grant No. CSTB2022BSXM-JCX0151], Graduate Innovation Program of Chongqing University of Science and Technology [Grant No. YKJCX2220702], Opening Fund of State Key Laboratory of Fire Science (HZ2023-KF07).

References

[1] Boukhelef, M., *et al.*, Numerical study of the injection conditions effect of the behavior of hydrogen-air diffusion flame, *Thermal science*, 26 (2022), 3741-3750

[2] Zuo, W., *et al.*, Parametric study of cavity on the performance of a hydrogen-fueled micro planar combustor for thermophotovoltaic applications, *Energy, 263*(2023), 126028

[3] Wang, Z. H., *et al.*, Flame morphologic characteristics of horizontally oriented jet fires impinging on a vertical plate: Experiments and theoretical analysis, *Energy, 264*(2023), 126210

[4] Zhang, B. Z., *et al.*, Numerical simulation and safety evaluation of multi-source leakage of buried product oil pipeline, *Energy Sources Part A-Recovery Utilization and Environmental Effects, 44*(2022), pp. 6737-6757

[5] Wang, C., *et al.*, Experimental study of flame morphology and size model of a horizontal jet flame impinging a wall, *Process Safety and Environmental Protection, 147*(2021), pp. 1009-1017

[6] Xie, K., *et al.*, Experimental study on the effect of spray cone angle on the characteristics of horizontal jet spray flame under sun-atmospheric pressure, *Thermal Science, 24* (2020), pp. 2941-2952.

[7] Zhang, X., *et al.*, Flame extension length and temperature profile in thermal impinging flow of buoyant round jet upon a horizontal plate, *Applied Thermal Engineering, 73*(2014), pp. 15-22

[8] Zhang, X., *et al.*, Flame lengths in two directions underneath a ceiling induced by line-source fire: An experimental study and global model, *Proceedings of the Combustion Institute, 38*(2021), pp. 4561-4568

[9] Zhang, X., *et al.*, Flame extension lengths beneath an inclined ceiling induced by rectangular-source fires, *Combustion and Flame, 176*(2017), pp. 349-357

[10] Wang, A., *et al.*, Experimental study on the flame extension and risk analysis of a diffusion impinging flame in confined compartment, *Journal of Fire Sciences, 39*(2021), pp. 285-308

[11] Hu, L. H., *et al.*, Flame heights of line-source buoyant turbulent non-premixed jets with air entrainment constraint by two parallel side walls, *Fuel 200*(2017), pp. 583-589

[12] Tao C. F., *et al.*, The investigation of flame length of buoyancy-controlled gas fire bounded by wall and ceiling, *Applied Thermal Engineering, 127*(2017), pp. 1172-1183

[13] Tao, C. F., *et al*., Experimental investigations on temperature profile and air entrainment of buoyancy-controlled jet flame from inclined nozzle bounded the wall, *Applied Thermal Engineering, 111*(2017), pp. 510-515
[14] Zhang, X. L., *et al*., Experimental study and analysis on flame lengths induced by wall-attached fire impinging upon an inclined ceiling, *Proceedings of the Combustion Institute, 37*(2019), pp. 3879-3887
[15] Palacios, A., Rengel, B., Computational analysis of vertical and horizontal jet fires, *Journal of Loss Prevention in the Process Industries, 65*(2020), 104096
[16] Houf, W., *et al*., Evaluation of barrier walls for mitigation of unintended releases of hydrogen, *International Journal of Hydrogen Energy, 35*(2010), pp. 4758-4775
[17] Houf, W. G., *et al*., A study of barrier walls for mitigation of unintended releases of hydrogen, *International Journal of Hydrogen Energy, 36*(2011), pp. 2520-2529
[18] Schefer, R. W., *et al*., Experimental evaluation of barrier walls for risk reduction of unintended hydrogen releases, *International Journal of Hydrogen Energy, 34*(2009), pp. 1590-1606
[19] Schefer, R. W., *et al*., Experimental investigation of hydrogen jet fire mitigation by barrier walls, *International Journal of Hydrogen Energy, 36*(2011), pp. 2530-2537
[20] Foroughi, V., *et al*., Thermal effects of a sonic jet fire impingement on a pipe, *Journal of Loss Prevention in the Process Industries, 71*(2021), 104449
[21] Wang Z. H., *et al*., Flame extension area and temperature profile of horizontal jet fire impinging on a vertical plate, *Process Safety and Environmental Protection, 147*(2021), pp. 547-558
[22] Huang, Y. B., *et al*., Computational investigation of flame extension height for horizontally oriented rectangular source jet fires impinging on a vertical plate, *Fire and Materials, 43*(2019), pp. 821-830
[23] Dong, B. Y., *et al.,* Temperature Profile of Thermal Impinging Flow Induced by Horizontally Oriented Rectangular Jet Flame Upon an Opposite Plate, *Journal of Thermal Science and Engineering Applications, 11*(2019), pp. 1-8
[24] Tang, F., *et al*., Flame characteristics and heat flux profile of a tank surface caused by horizontal gas leak jet fire impingement, *Fire Safety Journal, 134*(2022), 103709
[25] Palacios, A., *et al*., Thermal radiation from vertical jet fires, *Fire Safety Journal, 51*(2012), pp. 93-101
[26] Houf, W., Schefer, R., Analytical and experimental investigation of small-scale unintended releases of hydrogen, *International Journal of Hydrogen Energy, 33*(2008), pp. 1435-1444
[27] Tang, Z. H., *et al*., Study on the extension length of horizontal hydrogen jet fires under the action of water curtain, *Fuel, 322*(2022), 124254

Submitted: 28.03.2023.

Revised: 26.05.2023
Accepted: 29.05.2023.